# Chapter 2

# Structural Basis of Antibody–Antigen Interactions

**Eric J. Sundberg**

## Summary

Antibody molecules can be regarded as products of a protein engineering system for the generation of a virtually unlimited repertoire of complementary molecular surfaces. This extreme structural heterogeneity is required for recognition of the nearly infinite array of antigenic determinants. This chapter discusses the structures of antibodies and their specific recognition of antigens, the binding energetics of these interactions, the cross-reactivity and specificity of antibody–antigen interactions, the role of conformational flexibility in antigen recognition, and the structural basis of the antibody affinity maturation process.

**Key words:** Antibody, Antigen, X-ray crystallography, Binding energetics, Affinity maturation.

## 1. Structural Overview of Antibodies

The basic building blocks of antibodies are small protein domains, each composed of two antiparallel β-sheets and belonging to the immunoglobulin (Ig) fold superfamily *(1)*. **Fig. 1** provides an overview of the structural characteristics of Ig domains, how they are assembled to form functional antibodies, and how they generally recognize antigenic molecules. Antibody molecules are composed of two identical polypeptide chains of ~500 amino acids (the heavy or H chains) covalently linked through disulfide bridges to two identical polypeptide chains of roughly 250 residues (the light or L chains) (**Fig. 1a**). The H and L chains may be divided into N-terminal variable (V) and C-terminal constant (C) portions. Each H chain contains four or five Ig domains ($V_H$, $C_H1$, $C_H2$, $C_H3$ ± $C_H4$, depending on the antibody isotype), while each L chain consists of two such domains ($V_L$, $C_L$). The $V_L$ and $C_L$ domains are disulfide-linked with the $V_H$ and $C_H1$

Ulrich Reineke and Mike Schutkowski (eds.), *Methods in Molecular Biology, Epitope Mapping Protocols, vol. 524*

DOI: 10.1007/978-1-59745-450-6_2

domains, respectively, to form the Fab region (large oval, **Fig. 1a**) of the antibody, which is linked through a hinge region to the Fc domain, formed by noncovalent association of the $C_H2$–$3/4$ domains from both chains.

The variable domains of antibodies ($V_H$ and $V_L$), which together form what is referred to as the Fv (small oval, **Fig. 1a**), each contain three segments, which connect the β-strands and are highly variable in length and sequence *(4)*. These so-called complementarity-determining regions (CDRs) lie in close spatial proximity on the surface of the V domains and determine the conformation of the combining site (**Fig. 1b, c**). In this way, the CDRs confer specific binding activity to apical regions of the Ig domain. The central

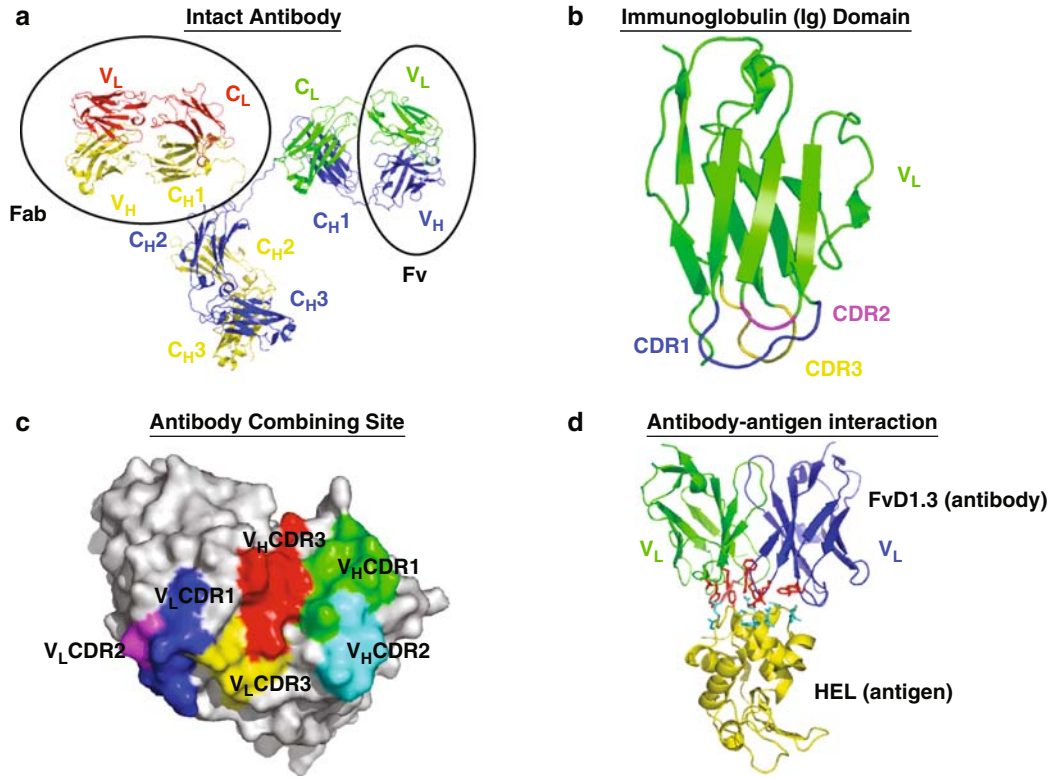


Fig. 1. Structural overview of antibodies. (**a**) Structure of the intact murine IgG2a monoclonal antibody, Mab231 *(2)*, including two light chains, each composed of a variable ($V_L$) and a constant ($C_L$) immunoglobulin (Ig) domain (*red* and *green*), and two heavy chains, each composed of a variable ($V_H$) and three constant ($C_H1$, $C_H2$, and $C_H3$) domains (*blue* and *yellow*) *(3)*. The common fragments, Fab (*large oval*) and Fv (*small oval*), are indicated. (**b**) Ribbon diagram of a single Ig domain, $V_L$, of Mab231 highlighting its antiparallel β-sheet secondary structure. The complementarity-determining region loops are marked, CDR1 (*blue*), CDR2 (*magenta*), and CDR3 (*yellow*). (**c**) Molecular surface of the antibody-combining site of Mab231 formed by the intersection of the apical regions of $V_L$ and $V_H$. The CDR loops provide a contiguous surface for antigen recognition. Colors are as follows: $V_L$CDR1 (*blue*), $V_L$CDR2 (*magenta*), $V_L$CDR3 (*yellow*), $V_H$CDR1 (*green*), $V_H$CDR2 (*cyan*), $V_H$CDR3 (*red*). (**d**) Ribbon diagram of the FvD1.3–hen egg lysozyme (HEL) antibody–antigen complex. Colors are as follows: HEL (*yellow*), D1.3 $V_L$ domain (*green*), and D1.3 $V_H$ domain (*blue*). Residues of HEL and D1.3 involved in interactions in the antigen–antibody interface are *cyan* and *red*, respectively (*see Color Plates*).

paradigm of antigen recognition is that the three-dimensional structure formed by the six CDRs recognizes and binds a complementary surface (epitope) on the antigen (**Fig.** 1d).

Although CDR loops are hypervariable, they adopt a limited number of canonical structures in antibodies *(5)*. Usage of the six CDR loops that confer antigen-binding specificity varies, especially for antibodies. Antibodies to smaller antigens, such as haptens and peptides, commonly do not utilize all six CDRs *(6, 7)*, while antiprotein antibodies generally do. Camelid antibodies that have no light chains *(8)* can nonetheless bind protein antigens with nanomolar affinities using as few as two CDR loops *(9)*. Cartilaginous fish, such as sharks, are the oldest living organisms that express components of the vertebrate adaptive immune system. These animals can recognize antigens using a single Ig domain that is similar to camelid heavy chain V domains *(10)*. Indeed, some of the contacts to various mammalian antibody CDR loops by protein antigens, while confirmed as structurally belonging to the molecular interface, are energetically meaningless. Additionally, both polyclonal and monoclonal antibodies (mAbs) raised against small (8- to 15-mer) peptides often bind to both the peptide and to the whole correlate protein, sometimes with higher affinity than antibodies raised directly against the latter *(11–13)*. Framework regions are commonly invoked in antigen recognition to varying degrees, and can comprise up to 15% of the buried surface area of an antibody–antigen complex *(14)*. The $V_H$CDRs, and $V_H$CDR3 in particular, generally make more extensive contacts than $V_L$CDRs, and the geometrical center of the antibody–antigen interface tends to lie near $V_H$CDR3. There exists a strong correlation between residues that do not form contacts with antigen and those residues that are important in defining the canonical backbone structures of the CDR loops *(15)*. These residues tend to pack internally and are therefore less exposed on the antibody-combining site surface.

Antibody–antigen complexes exhibit a high degree of both shape and chemical complementarity at their interacting surfaces *(16)*. The combined solvent-accessible surfaces buried in antiprotein antibody–antigen complexes range from ~1,400 to 2,300 Å$^2$, with roughly equal contributions from antigen and antibody, while smaller antigens, such as haptens and peptides, generally bury less overall surface area when bound to the antibody. The surface topography of the antigen-contacting surface, as well as other general structural features, of antibodies can vary significantly according to antigen size *(17)*. While the percentage of the antigen surface buried in the interface with the antibody is always high and their surfaces are complementary, the antibody contact surface becomes more concave as the antigen becomes smaller. Thus, although the combining sites of antibodies that recognize large protein antigens are generally planar, and are often more

planar than a number of other types of protein–protein interfaces *(18)*, antibodies that recognize medium-sized antigens, such as peptides, DNA, and carbohydrates, often have a grooved antigen-contacting surface, while even smaller antigens (haptens) are recognized by antibodies with distinct cavities *(19)*. A common feature of antipeptide antibody–antigen interactions is a β-turn motif of the peptide buried deeply into the combining site *(20–22)*. The amount of surface area on the antibody molecule buried by the antigen decreases with antigen size, as less of the antibody surface is utilized to envelop the smaller antigens. Large antigens often contact antibody residues at the edge of the combining site and interact with the more apical portions of the CDR loops, while the interactions of smaller antigens are more restricted to the central portion of the antibody-combining site *(17)*.

## 2. Binding Energetics of Antigen Recognition

There exists a functional affinity window for antigen recognition. Antibodies undergo affinity maturation upon encountering their specific antigens (addressed later in this chapter). Below, the binding properties of fully matured antibodies are discussed.

Most mature antibodies have affinities for their specific antigens in the range of $10^7 - 10^8$ $M^{-1}$, although many functional antibodies that recognize carbohydrates and bacterial polysaccharides fail to reach affinity levels of $10^6$ $M^{-1}$. It has been proposed *(23)* that, owing to diffusion rates and the residence time required for antibody internalization controlling on- and off-rates, there exists an affinity ceiling for antibody–antigen interactions of ~$10^{10}$ $M^{-1}$. Antibodies with antigen affinities above this threshold, presumably, would possess no further advantage over their lower affinity counterparts in the antibody selection process in vivo. The existence of this affinity ceiling has been demonstrated for antigen-specific B-cell transfectants, and more important, an affinity window for effective B-cell response has been revealed for which a minimum affinity of $10^6$ $M^{-1}$ and half-life of 1 s were required for detectable B-cell triggering that reached a plateau for affinities beyond $10^{10}$ $M^{-1}$ *(24)*. Not surprisingly, when primary response antibodies exhibit affinities for their specific antigens approaching this affinity ceiling, they neither require nor undergo further affinity maturation *(25)*. This effective affinity window, however, appears to shift to a range of lower affinities, with an affinity ceiling of ~$10^6$ $M^{-1}$, when the antigen is in particulate form, presumably because of avidity effects. Conversely, the range of the affinity window for extraction of antigen from a noninternalizable surface remains quite broad with an affinity ceiling similar to that

of soluble antigens *(26)*. Antigens in these nonsoluble forms are thought to more closely mimic the properties of antigens in vivo.

As the overall affinity of antibody–antigen interactions can vary by several orders of magnitude, so too can the kinetics of these interactions. In a number of kinetic analyses of antiprotein antibodies *(27–30)*, both association and dissociation rates vary by greater than 2 log-fold. Thermodynamically, the formation of many antibody–antigen complexes reflects an enthalpically driven process with some compensating negative entropy component, alluding to an important role for the release of bound water molecules. In fact, a strong correlation between decreases in water activity and association constants in an antibody–protein-antigen complex has been observed by calorimetric binding analyses done in the presence of cosolutes with polarities lower than that of water *(31)*. Although other antibody–protein-antigen *(32)* and antibody–carbohydrate-antigen *(33)* interactions also appear enthalpically driven, this may not be the general rule for antibody–antigen associations because of the limited number of such systems whose thermodynamics have been rigorously determined. In accordance with the significance of water activity on antigen recognition, antibodies binding to both protein and hapten antigens have exhibited a thermodynamic dependence on the solvent pH and ionic strength *(27, 34–36)*.

## 3. Antigen Cross-Reactivity and Specificity

Although specific recognition of foreign vs. self material is tantamount to proper immune function, antibodies and TCRs are frequently involved in spurious interaction events. While antibodies are commonly highly specific for a single antigen, it is not at all uncommon for them to cross-react with many, structurally similar, yet distinct, antigenic molecules. In some cases, cross-reactivity has been shown to be involved in autoimmune and allergic reactions *(37, 38)*.

Certain antibodies can bind better to antigens not used in challenging the immune system than to the original immunogen, a phenomenon known as heteroclitic binding. For example, the mAb D11.15, raised against hen egg lysozyme (HEL), interacts with higher affinity with several other avian lysozymes, and the molecular basis for this cross-reactivity has been elucidated *(6)*. FvD11.15 binds eight different avian lysozymes, and all of these exhibit high affinities for the antibody. Two of these, pheasant egg-white lysozyme and guinea fowl egg-white lysozyme, exceed the affinity of the interaction with HEL, and another, Japanese quail egg-white lysozyme, exhibits a slightly lower affinity than that

of HEL. Crystal structures of these antibody–antigen complexes reveal that distinct structural mechanisms, such as displacement of a loop region or an increase in hydrophobic surface on the antigen, are the cause of these heteroclitic binding events. Another anti-HEL antibody, D1.3, binds only its immunogen and one other avian lysozyme, bobwhite quail egg-white lysozyme, with high affinity. Much of the sequence variability between these eight avian lysozymes occurs at HEL residue Gln-121. For the highly cross-reactive D11.15, lysozyme residue 121 is located at the periphery of the antigenic epitope. Conversely, for the highly specific D1.3, this residue is located centrally to the binding interface and acts as a hot spot in binding for the D1.3–HEL complex *(39)*.

Anti-idiotopic antibodies *(40, 41)* recognize an antigenic determinant that is unique to an antibody or group of antibodies, or idiotope. An idiotope is defined functionally by the interaction of an anti-idiotopic antibody (Ab2) with an antibody (Ab1) bearing the idiotope. Conventional Ab2 antibodies recognize idiotopes outside of the antibody-combining site paratope, while internal image Ab2 antibodies are able to mimic the molecular surface encountered by Ab1, thereby mimicking stereochemically the antigen specific for Ab1. Numerous efforts have been made to use these molecular mimics as therapeutics, similar to vaccines. The D1.3 antibody binds to two structurally distinct ligands – its cognate antigen, HEL, and the anti-idiotypic antibody E5.2 – and these interactions exhibit molecular mimicry. The crystal structures of the complexes formed by FvD1.3 with both HEL *(42)* and FvE5.2 *(43, 44)* have been determined under high resolution. FvD1.3 contacts HEL and FvE5.2 through essentially the same set of combining site residues and most of the same atoms. Of the 18 FvD1.3 residues that contact FvE5.2 and the 17 that contact HEL, 14 are in contact with both FvE5.2 and HEL. These 14 FvD1.3 residues make up 75% of the total contact area with FvE5.2 and 87% of that with HEL. Furthermore, the positions of the atoms of FvE5.2 that contact FvD1.3 are close to those of HEL that contact FvD1.3, and 6 of the 12 hydrogen bonds in the FvD1.3–FvE5.2 interface are structurally equivalent to hydrogen bonds in the FvD1.3–HEL interface.

Perhaps the most striking example of antigen cross-reactivity of an antibody is that of SPE7, a mouse monoclonal IgE antibody raised against the hapten 2,4-dinitrophenol (DNP), to which it binds with relatively high affinity ($K_D$ = 20 nM) *(45)*. SPE7 also binds to other small molecules with widely ranging affinities *(46)*, as well as to a structurally unrelated protein antigen, Trx-Shear3, selected using a directed evolution strategy. The Fv portion of this antibody crystallized in two different conformations in its unbound form, one of which resembled the structure of the antibody when bound by DNP any of a number of small

molecules, while the other resembled the antibody structure in its protein-antigen-bound form *(47)*. Analysis of the presteady-state kinetics of complex formation between SPE7 and DNP revealed that the antibody exists in two distinct isomers, only one of which is capable of binding to the small molecule antigens. Thus, there appears to exist an equilibrium between preexisting SPE7 isomers that have the ability to bind different antigens. This diversity in the conformational ensemble space in the unbound form may serve to increase the repertoire of functional antibodies.

## 4. Conformational Flexibility in Antibody–Antigen Interactions

The kinetics of antibody–antigen interactions is commonly temperature-dependent. In some cases this may be indicative of the structural plasticity involved in antigen binding. Indeed, the binding kinetics of several anti-HEL antibodies have been shown to conform to a two-state model describing induced fit, with distinct association steps for molecular encounter and docking *(48, 49)*. Although numerous hypotheses concerning the correlation between antibody flexibility and signaling have been proposed over the years, the establishment of molecular flexibility as a component of signaling, beyond the antigen recognition event, remains elusive.

For smaller antigens, notably peptides and DNA, antibody plasticity is generally more pronounced than for protein antigens, although associations with the latter commonly involve a nominal degree of molecular flexibility and cannot necessarily be classified as "lock-and-key" interactions. Two types of backbone movements within the antibody-combining site have commonly been observed upon antibody–antigen complex formation, including concerted movements of multiple residue segments of CDR loops and more heterogeneous rearrangements of CDR residues. For example, upon binding antigen, heavy chain CDR loops in the antipeptide Fab8F5 undergo essentially rigid-body movements in which the unliganded loop conformations are conserved, while changes in the main chain conformation of the light chain are insignificant *(50)*. The culmination of concerted heavy chain CDR movements towards the light chain reduces the volume of the antigen-binding site by some 3% relative to the unbound Fab8F5. Other examples of segments of CDR loops moving en masse towards antigen have been observed *(21)*. In Fab17/9, a significant rearrangement of the $V_H$CDR3 loop is induced by binding of its peptide antigen, for which the largest backbone changes are 5 Å *(20)*. Restructuring of CDR loop regions from both the heavy and light chains of the anti-DNA antibody FabBV04–01 has also

been observed *(51)*. Induced CDR loop movements upon antigen binding seem to be less extreme for antiprotein antibodies. Generally, these are small, concerted displacements of less than 3 Å *(42, 52–56)*.

Molecular flexibility is not limited to a single side of the interface, as a number of structural studies have shown varying degrees of protein plasticity for antigens upon recognition by antibodies. HEL can be crystallized in several space groups *(57–59)*. Comparison of the structures reveals significant flexibility of several loops at the molecular surface, including a number of Cα atom displacements greater than 3 Å between HEL molecules from different space groups. Between crystal structures of HEL bound to different antibodies, some main chain movements become more pronounced *(6, 42, 54, 60)*. Increased antigen flexibility, however, is not always beneficial to epitope recognition by antibodies. For instance, in order to produce mimics of the N-terminal sequence of a transforming growth factor alpha epitope recognized by the mAb tAb2, peptides required cyclicization to constrain their conformations to ones that are suitable for binding *(61)*.

## 5. Antibody Affinity Maturation

The function of the immune system is dependent on the recognition of essentially any antigenic material, yet the structural diversity of antigens greatly outweighs the genetic diversity encoded by immune system genes. Thus, molecular recognition of diverse antigens is accomplished by producing antibodies with specificity for almost any antigen via recombination and imprecise joining of antibody gene segments. This focuses molecular diversity at the contiguous molecular surface formed by the CDR loops, the combining site for antigen recognition. This results in germline antibodies of relatively low affinity and specificity *(62)*. This junctional diversity in the primary repertoire can produce CDR loops of different lengths and varying structures *(63, 64)*.

The affinity requirements for functional antibodies (approximately $K_D$s in the nanomolar range) necessitate a secondary process for improving affinity and specificity once diversity has been established. The somatic hypermutation of antibody V regions spreads structural diversity generated by gene segment recombination to regions at the periphery of the binding site *(65)*. Selective expansion of antibody clones on the basis of antigen affinity produces mature antibodies that are high in both affinity and specificity *(66)*. Somatic hypermutation is primarily a point mutation process in gene regions that are highly conserved in the primary repertoire that can result, at times, in codon insertions

or deletions *(65)*. It has been shown that the presence or absence of certain $V_H$CDR3 junctional amino acids can determine the affinity maturation pathway of an antibody by biasing subsequent amino acid replacements by somatic hypermutation *(67)* and that these effects are correlated to the structure and flexibility of the $V_H$CDR3 loop in the germline antibodies *(68)*.

Structural and energetic studies comparing germline and mature antibodies bound to the same antigen have advanced our understanding of the effects of somatic hypermutation on antibody affinity maturation. The mature Fab48G7 and its germline counterpart, Fab48G7g, both bind a nitrophenyl phosphonate transition-state analog, but with a 30,000-fold difference in affinity, primarily due to a decrease in the dissociation rate *(69)*. The sequence differences between the Fabs are limited to nine somatic hypermutations, six in $V_H$ and three in $V_L$, located up to 15 Å from the bound hapten. Crystal structures of the unliganded germline Fab48G7g and its complex with hapten *(69)* reveal large conformational changes induced upon antigen binding, while crystal structures of the mature Fab48G7 *(70, 71)* in its free and hapten-bound forms exhibit very few conformational changes upon complex formation. The conformational changes induced upon antigen binding by Fab48G7g are later observed in the mature Fab structure even in the absence of antigen, and thus it appears, at least in the case of the Fab48G7 system, that the affinity maturation process is driven in large part by a mechanism of preorganizing the antibody-combining site into a conformation that is favorable for binding its hapten antigen.

Through the introduction of forward and back site-directed mutations in the germline and mature Fabs and measurements of binding affinities, the effects of the nine somatic hypermutations on the affinity maturation pathway of Fab48G7 have been dissected *(72)*. In this system, the effect on binding of the individual mutations was either positive or neutral, yet their additive changes in affinity were not equal to the overall change in affinity between the germline and mature Fabs. Double mutations revealed a high degree of cooperativity between mutations, not only between individually neutral mutations but also between even the two most positive individual mutations.

Cooperativity between somatic hypermutations, however, does not appear to be a required mechanism for affinity maturation. For Fab39-A11, which catalyzes a Diels–Alder reaction, only two somatic mutations exist between the germline and mature counterparts, of which only one contributes the majority of binding affinity to mature Fab *(73)*. Another catalytic antibody, AZ-28, which catalyzes an oxy-Cope rearrangement, has six somatic mutations, five of which contribute to differences in affinity between germline and mature antibodies in a strictly additive way *(74)*. In the affinity maturation of an antiprotein antibody,

FvD1.3, the five somatic hypermutations have also been shown to be energetically additive *(75)*. In this system, changes in antigen affinity are dominated by the only mutated amino acid that is in direct contact with the antigen, HEL.

The quantity and cooperativity of somatic hypermutations may be dependent on the affinity differences between the germline and mature antibodies. The affinity discrepancy between Fab48G7 and Fab48G7g is 30,000-fold *(69)*, while FabAZ-28, with only five significant somatic mutations has an antigen affinity only 40-fold greater than its germline counterpart *(74)*. Furthermore, Fab39-A11 and Fab39-A11g, with only one significant amino acid difference, both bind nine haptens, for most of which the difference in affinity is within an order of magnitude *(73)*. Germline and mature FvD1.3 also differ by only five amino acids and by 60-fold in affinity *(75)*. If one considers that mature antibodies must break a minimum affinity threshold for antigen binding through a limited number of somatic mutations to be functional in vivo, then it follows that the number of somatic mutations will increase as the difference in affinities between germline and mature antibodies gets larger and cooperativity between the somatic mutations will be utilized in cases where the affinity maturation process must overcome extreme germline–mature affinity discrepancies. Precise affinity ranges for the lack or presence of cooperativity associated with somatic hypermutation may or may not actually exist.

Recently, the crystal structures of four closely related anti-HEL antibodies (HyHEL8, HyHEL10, HyHEL26, and HyHEL63), representing different stages of affinity maturation, were determined bound to the same site on HEL *(76)*, revealing that enhanced binding is achieved by the burial of increasing amounts of apolar surface, at the expense of polar surface, accompanied by improved shape complementarity. The increase in hydrophobic interactions, which can fully account for the 30-fold affinity improvement in these anti-HEL antibodies according to an experimental estimate of the hydrophobic effect in protein–protein interactions *(77)*, is the consequence of subtle, yet highly correlated, structural rearrangements in antibody residues at the periphery of the interface with the antigen, adjacent to the central energetic hot spot, whose structure remains unaltered. While increasing hydrophobic interactions and improving the fit at peripheral sites that have not been optimized for binding, and whose plasticity and ability to accommodate mutations render them permissive to such optimization, constitute effective strategies for maturing antiprotein antibodies, other, as yet unobserved, mechanisms may be utilized by various antibodies for affinity maturation.

Some of the energetic factors involved in the preorganization of mature antibodies through somatic hypermutation of germline antibodies have been elucidated recently using surface plasmon

resonance techniques in which different binding characteristics at various temperatures of the same complex provide information relative to the enthalpic and entropic contributions to the interaction. The affinities of panels of early primary and secondary response mAbs for a model synthetic 40-mer peptide were determined at two temperatures *(78)*. The effects of temperature on the dissociation step of the interaction were similar for mAbs in both panels, while opposite temperature effects on association were observed for each panel of mAbs. For primary mAbs, complex association was enthalpically highly favorable but entropically unfavorable, while dissociation was enthalpically unfavorable and entropically favorable. The equilibrium binding for primary mAbs was enthalpically driven with a large entropic cost of complex formation, resulting in relatively low affinity. Conversely, in secondary mAbs, association was enthalpically unfavorable but the entropic costs had been reduced markedly. Because the dissociation step of the reaction was similar to that for primary mAbs, equilibrium binding in the secondary mAbs was essentially independent of enthalpy effects, and instead, was driven by entropic changes. Thus, the relatively high affinity of the secondary mAbs is derived exclusively from the nearly complete abolishment of any entropic costs of complex association in comparison to the primary mAbs. While these experiments seem to confirm the idea of antibody affinity maturation through paratope preorganization, at least for an antipeptide antibody, it is intriguing to note that the increased affinities in the antihapten Fab48G7 and the antiprotein FvD1.3 systems derive nearly entirely from decreases in the dissociation phases of the reactions *(69, 75)*. Although similar experiments examining enthalpy and entropy effects on antigen binding to germline and mature Fab48G7 and FvD1.3 have not been done, it is likely that these types of experiments would reveal that these complexes are stabilized because of large entropic barriers to dissociation in the mature vs. germline antibodies.

## References


1. Amzel, L. M., and Poljak, R. J. (1979) Three-dimensional structure of immunoglobulins. *Annu. Rev. Biochem.* 48, 961–997.
2. Harris, L. J., Larson, S. B., Hasel, K. W., and McPherson, A. (1997) Refined structure of an intact IgG2a monoclonal antibody. *Biochemistry* 36, 1581–1597.
3. Harris, L. J., Skaletsky, E., and McPherson, A. (1998) Crystallographic structure of an intact IgG1 monoclonal antibody. *J. Mol. Biol.* 275, 861–872.
4. Wu, T. T., and Kabat, E. A. (1970) An analysis of the sequences of the variable regions of Bence Jones proteins and myeloma light chains and their implications for antibody complementarity. *J. Exp. Med.* 132, 211–250.
5. Al-Lazikani, B., Lesk, A. M., and Chothia, C. (1997) Standard conformations for the canonical structures of immunoglobulins. *J. Mol. Biol.* 273, 927–948.
6. Chitarra, V., Alzari, P. M., Bentley, G. A., Bhat, T. N., Eiselé, J. L., Houdusse, A., Lescar,

J., Souchon, H., and Poljak, R. J. (1993) Three-dimensional structure of a heteroclitic antigen–antibody cross-reaction complex. *Proc. Natl. Acad. Sci. USA* 90, 7711–7715.

7. Wilson, I. A., and Stanfield, R. L. (1993) Antibody–antigen interactions. *Curr. Opin. Struct. Biol.* 3, 113–118.
8. Hamers-Casterman, C., Atarhouch, T., Muyldermans, S., Robinson, G., Hamers, C., Songa, E. B., Bendahman, N., and Hamers, R. (1993) Naturally occurring antibodies devoid of light chains. *Nature* 363, 446–448.
9. Decanniere, K., Desmyter, A., Lauwereys, M., Ghahroudi, M. A., Muyldermans, S., and Wyns, L. (1999) A single-domain antibody fragment in complex with RNase A: non-canonical loop structures and nanomolar affinity using two CDR loops. *Struct. Fold. Des.* 7, 361–370.
10. Stanfield, R. L., Dooley, H., Flajnik, M. F., and Wilson, I. A. (2004) Crystal structure of a shark single-domain antibody V region in complex with lysozyme. *Science* 305, 1770–1773.
11. Chersi, A., Galati, R., Ogino, T., Butler, R. H., and Tanigaki, N. (2002) Anti-peptide antibodies that recognize conformational differences of HLA class I intracytoplasmic domains. *Hum. Immunol.* 63, 731–741.
12. Hewer, R., and Meyer, D. (2003) Peptide immunogens based on the envelope region of HIV-1 are recognized by HIV/AIDS patient polyclonal antibodies and induce strong humoral immune responses in mice and rabbits. *Mol. Immunol.* 40, 327–335.
13. Metaxas, A., Tzartos, S., and Liakopoulou-Kyriakide, M. (2002) The production of anti-hexapeptide antibodies which recognize the S7, L6 and L13 ribosomal proteins of *Escherichia coli*. *J. Pept. Sci.* 8, 118–124.
14. Wilson, I. A., and Stanfield, R. L. (1994) Antibody–antigen interactions: new structures and new conformational changes. *Curr. Opin. Struct. Biol.* 4, 857–867.
15. Chothia, C., Lesk, A. M., Tramontano, A., Levitt, M., Smith-Gill, S. J., Air, G., Sheriff, S., Padlan, E. A., Davies, D., and Tulip, W. R. (1989) Conformations of immunoglobulin hypervariable regions. *Nature* 342, 877–883.
16. Conte, L. L., Chothia, C., and Janin, J. (1999) The atomic structure of protein–protein recognition sites. *J. Mol. Biol.* 285, 2177–2198.
17. MacCallum, R. M., Martin, A. C., and Thornton, J. M. (1996) Antibody–antigen interactions: contact analysis and binding site topography. *J. Mol. Biol.* 262, 732–745.
18. Jones, S., and Thornton, J. M. (1996) Principles of protein–protein interactions. *Proc. Natl. Acad. Sci. USA* 93, 13–20.
19. Webster, D. M., Henry, A. H., and Rees, A. R. (1994) Antibody–antigen interactions. *Curr. Opin. Struct. Biol.* 4, 123–129.
20. Rini, J. M., Schulze-Gahmen, U., and Wilson, I. A. (1992) Structural evidence for induced fit as a mechanism for antibody–antigen recognition. *Science* 255, 959–965.
21. Stanfield, R. L., Fieser, T. M., Lerner, R. A., and Wilson, I. A. (1990) Crystal structures of an antibody to a peptide and its complex with peptide antigen at 2.8 Å. *Science* 248, 712–719.
22. Garcia, K. C., Ronco, P. M., Verroust, P. J., Brünger, A. T., and Amzel, L. M. (1992) Three-dimensional structure of an angiotensin II-Fab complex at 3 Å: hormone recognition by an anti-idiotypic antibody. *Science* 257, 502–507.
23. Foote, J., and Eisen, H. N. (1995) Kinetic and affinity limits on antibodies produced during immune responses. *Proc. Natl. Acad. Sci. USA* 92, 1254–1256.
24. Batista, F. D., and Neuberger, M. S. (1998) Affinity dependence of the B cell response to antigen: a threshold, a ceiling, and the importance of off-rate. *Immunity* 8, 751–759.
25. Roost, H. P., Bachmann, M. F., Haag, A., Kalinke, U., Pliska, V., Hengartner, H., and Zinkernagel, R. M. (1995) Early high-affinity neutralizing anti-viral IgG responses without further overall improvements of affinity. *Proc. Natl. Acad. Sci. USA* 92, 1257–1261.
26. Batista, F. D., and Neuberger, M. S. (2000) B cells extract and present immobilized antigen: implications for affinity discrimination. *EMBO J.* 19, 513–520.
27. Xavier, K. A., McDonald, S. M., McCammon, J. A., and Willson, R. C. (1999) Association and dissociation kinetics of bobwhite quail lysozyme with monoclonal antibody HyHEL-5. *Protein Eng.* 12, 79–83.
28. Gerstner, R. B., Carter, P., and Lowman, H. B. (2002) Sequence plasticity in the antigen-binding site of a therapeutic anti-HER2 antibody. *J. Mol. Biol.* 321, 851–862.
29. Rajpal, A. and Kirsch, J. F. (2000) Role of the minor energetic determinants of chicken egg white lysozyme (HEWL) to the stability of the HEWL antibody scFv-10 complex. *Proteins* 40, 49–57.
30. England, P., Bregegere, F., and Bedouelle, H. (1997) Energetic and kinetic contributions of contact residues of antibody D1.3 in the interaction with lysozyme. *Biochemistry* 36, 164–172.
31. Goldbaum, F. A., Schwarz, F. P., Eisenstein, E., Cauerhff, A., Mariuzza, R. A., and Poljak, R. J. (1996) The effect of water activity on the association constant and the enthalpy of reaction between lysozyme and the specific

antibodies D1.3 and D44.1. *J. Mol. Recognit.* 9, 6–12.

32. Kelley, R. F., O'Connell, M. P., Carter, P., Presta, L., Eigenbrot, C., Covarrubias, M., Snedecor, B., Bourell, J. H., and Vetterlein, D. (1992) Antigen binding thermodynamics and antiproliferative effects of chimeric and humanized anti-p185HER2 antibody Fab fragments. *Biochemistry* 31, 5434–5441.
33. Sigurskjold, B. W., Altman, E., and Bundle, D. R. (1991) Sensitive titration microcalorimetric study of the binding of Salmonella O-antigenic oligosaccharides by a monoclonal antibody. *Eur. J. Biochem.* 197, 239–246.
34. Gibas, C. J., Subramaniam, S., McCammon, J. A., Braden, B. C., and Poljak, R. J. (1997) pH dependence of antibody/lysozyme complexation. *Biochemistry* 36, 15599–15614.
35. Omelyanenko, V. G., Jiskoot, W., and Herron, J. N. (1993) Role of electrostatic interactions in the binding of fluorescein by anti-fluorescein antibody 4–4–20. *Biochemistry* 32, 10423–10429.
36. De Genst, E., Areskoug, D., Decanniere, K., Muyldermans, S., and Andersson, K. (2002) Kinetic and affinity predictions of a protein–protein interaction using multivariate experimental design. *J. Biol. Chem.* 277, 29897–29907.
37. Kaplan, M. H., and Meyeserian, M. (1962) An immunological cross-reaction between group-A streptococcal cells and human heart tissue. *Lancet* 1, 706–710.
38. Oldstone, M. B. (1998) Molecular mimicry and immune-mediated diseases. *FASEB J.* 12, 1255–1265.
39. Dall'Acqua, W., Goldman, E. R., Eisenstein, E., and Mariuzza, R. A. (1996) A mutational analysis of the binding of two different proteins to the same antibody. *Biochemistry* 35, 9667–9676.
40. Poljak, R. J. (1994) An idiotope–anti-idiotope complex and the structural basis of molecular mimicking. *Proc. Natl. Acad. Sci. USA* 91, 1599–1600.
41. Pan, Y., Yuhasz, S. C., and Amzel, L. M. (1995) Anti-idiotypic antibodies: biological function and structural studies. *FASEB J.* 9, 43–49.
42. Bhat, T. N., Bentley, G. A., Boulot, G., Greene, M. I., Tello, D., Dall'Acqua, W., Souchon, H., Schwarz, F. P., Mariuzza, R. A., and Poljak, R. J. (1994) Bound water molecules and conformational stabilization help mediate an antigen–antibody association. *Proc. Natl. Acad. Sci. USA* 91, 1089–1093.
43. Braden, B. C., Fields, B. A., Ysern, X., Dall'Acqua, W., Goldbaum, F. A., Poljak, R. J., and Mariuzza, R. A. (1996) Crystal structure of an Fv-Fv idiotope-anti-idiotope complex at 1.9 Å resolution. *J. Mol. Biol.* 264, 137–151.
44. Fields, B. A., Goldbaum, F. A., Ysern, X., Poljak, R. J., and Mariuzza, R. A. (1995) Molecular basis of antigen mimicry by an anti-idiotope. *Nature* 374, 739–742.
45. Eshhar, Z., Ofarim, M., and Waks, T. (1980) Generation of hybridomas secreting murine reaginic antibodies of anti-DNP specificity. *J. Immunol.* 124, 775–780.
46. Varga, J. M., Kalchschmid, G., Klein, G. F., and Fritsch, P. (1991) Mechanism of allergic cross-reactions – I. Multispecific binding of ligands to a mouse monoclonal anti-DNP IgE antibody. *Mol. Immunol.* 28, 641–654.
47. James, L. C., Roversi, P., and Tawfik, D. S. (2003) Antibody multispecificity mediated by conformational diversity. *Science* 299, 1362–1367.
48. Li, Y., Lipschultz, C. A., Mohan, S., and Smith-Gill, S. J. (2001) Mutations of an epitope hot-spot residue alter rate limiting steps of antigen–antibody protein–protein associations. *Biochemistry* 40, 2011–2022.
49. Lipschultz, C. A., Li, Y., and Smith-Gill, S. J. (2000) Experimental design for analysis of complex kinetics using surface plasmon resonance. *Methods* 20, 310–318.
50. Tormo, J., Blaas, D., Parry, N. R., Rowlands, D., Stuart, D., and Fita, I. (1994) Crystal structure of a human rhinovirus neutralizing antibody complexed with a peptide derived from viral capsid protein VP2. *EMBO J.* 13, 2247–2256.
51. Herron, J. N., He, X. M., Ballard, D. W., Blier, P. R., Pace, P. E., Bothwell, A. L., Voss, E. W., Jr., and Edmundson, A. B. (1991) An autoantibody to single-stranded DNA: comparison of the three-dimensional structures of the unliganded Fab and a deoxynucleotide–Fab complex. *Proteins* 11, 159–175.
52. Prasad, G. S., Earhart, C. A., Murray, D. L., Novick, R. P., Schlievert, P. M., and Ohlendorf, D. H. (1993) Structure of toxic shock syndrome toxin 1. *Biochemistry* 32, 13761–13766.
53. Mylvaganam, S. E., Paterson, Y., and Getzoff, E. D. (1998) Structural basis for the binding of an anti-cytochrome c antibody to its antigen: crystal structures of FabE8-cytochrome c complex to 1.8 Å resolution and FabE8 to 2.26 Å resolution. *J. Mol. Biol.* 281, 301–322.
54. Li, Y., Li, H., Smith-Gill, S. J., and Mariuzza, R. A. (2000) Three-dimensional structures of the free and antigen-bound Fab from monoclonal antilysozyme antibody HyHEL-63. *Biochemistry* 39, 6296–6309.
55. Braden, B. C., Souchon, H., Eiselé, J. L., Bentley, G. A., Bhat, T. N., Navaza, J., and Poljak, R. J. (1994) Three-dimensional structures of the free and the antigen-complexed

Fab from monoclonal anti-lysozyme antibody D44.1. *J. Mol. Biol.* 243, 767–781.

56. Faelber, K., Kirchhofer, D., Presta, L., Kelley, R. F., and Muller, Y. A. (2001) The 1.85 Å resolution crystal structures of tissue factor in complex with humanized Fab D3h44 and of free humanized Fab D3h44: revisiting the solvation of antigen combining sites. *J. Mol. Biol.* 313, 83–97.
57. Kurinov, I. V., and Harrison, R. W. (1995) The influence of temperature on lysozyme crystals. Structure and dynamics of protein and water. *Acta Crystallogr. D* 51, 98–109.
58. Harata, K. (1994) X-ray structure of a monoclinic form of hen egg-white lysozyme crystallized at 313 K. Comparison of two independent molecules. *Acta Crystallogr. D* 50, 250–257.
59. Ramanadham, M., Sieker, L. C., and Jensen, L. H. (1990) Refinement of triclinic lysozyme: II. The method of stereochemically restrained least squares. *Acta Crystallogr. B* 46, 63–69.
60. Padlan, E. A., Silverton, E. W., Sheriff, S., Cohen, G. H., Smith-Gill, S. J., and Davies, D. R. (1989) Structure of an antibody–antigen complex: crystal structure of the HyHEL-10 Fab-lysozyme complex. *Proc. Natl. Acad. Sci. USA* 86, 5938–5942.
61. Hahn, M., Winkler, D., Welfle, K., Misselwitz, R., Welfle, H., Wessner, H., Zahn, G., Scholz, C., Seifert, M., Harkins, R., Schneider-Mergener, J., and Höhne, W. (2001) Cross-reactive binding of cyclic peptides to an anti-TGFalpha antibody Fab fragment: an X-ray structural and thermodynamic analysis. *J. Mol. Biol.* 314, 293–309.
62. Tonegawa, S. (1983) Somatic generation of antibody diversity. *Nature* 302, 575–581.
63. Chothia, C., Lesk, A. M., Gherardi, E., Tomlinson, I. M., Walter, G., Marks, J. D., Llewelyn, M. B., and Winter, G. (1992) Structural repertoire of the human VH segments. *J. Mol. Biol.* 227, 799–817.
64. Tomlinson, I. M., Cox, J. P., Gherardi, E., Lesk, A. M., and Chothia, C. (1995) The structural repertoire of the human V kappa domain. *EMBO J.* 14, 4628–4638.
65. Tomlinson, I. M., Walter, G., Jones, P. T., Dear, P. H., Sonnhammer, E. L., and Winter, G. (1996) The imprint of somatic hypermutation on the repertoire of human germline V genes. *J. Mol. Biol.* 256, 813–817.
66. Rajewsky, K. (1996) Clonal selection and learning in the antibody system. *Nature* 381, 751–758.
67. Furukawa, K., Akasako-Furukawa, A., Shirai, H., Nakamura, H., and Azuma, T. (1999) Junctional amino acids determine the maturation pathway of an antibody. *Immunity* 11, 329–338.
68. Furukawa, K., Shirai, H., Azuma, T., and Nakamura, H. (2001) A role of the third complementarity-determining region in the affinity maturation of an antibody. *J. Biol. Chem.* 276, 27622–27628.
69. Wedemayer, G. J., Patten, P. A., Wang, L. H., Schultz, P. G., and Stevens, R. C. (1997) Structural insights into the evolution of an antibody combining site. *Science* 276, 1665–1669.
70. Wedemayer, G. J., Wang, L. H., Patten, P. A., Schultz, P. G., and Stevens, R. C. (1997) Crystal structures of the free and liganded form of an esterolytic catalytic antibody. *J. Mol. Biol.* 268, 390–400.
71. Patten, P. A., Gray, N. S., Yang, P. L., Marks, C. B., Wedemayer, G. J., Boniface, J. J., Stevens, R. C., and Schultz, P. G. (1996) The immunological evolution of catalysis. *Science* 271, 1086–1091.
72. Yang, P. L., and Schultz, P. G. (1999) Mutational analysis of the affinity maturation of antibody 48G7. *J. Mol. Biol.* 294, 1191–1201.
73. Romesberg, F. E., Spiller, B., Schultz, P. G., and Stevens, R. C. (1998) Immunological origins of binding and catalysis in a Diels-Alderase antibody. *Science* 279, 1929–1933.
74. Ulrich, H. D., Mundorff, E., Santarsiero, B. D., Driggers, E. M., Stevens, R. C., and Schultz, P. G. (1997) The interplay between binding energy and catalysis in the evolution of a catalytic antibody. *Nature* 389, 271–275.
75. England, P., Nageotte, R., Renard, M., Page, A. L., and Bedouelle, H. (1999) Functional characterization of the somatic hypermutation process leading to antibody D1.3, a high affinity antibody directed against lysozyme. *J. Immunol.* 162, 2129–2136.
76. Li, Y., Li, H., Smith-Gill, S. J., and Mariuzza, R. A. (2003) X-ray snapshots of the maturation of an antibody response to a protein antigen. *Nat. Struct. Biol.* 10, 482–488.
77. Sundberg, E. J., Urrutia, M., Braden, B. C., Isern, J., Tsuchiya, D., Fields, B. A., Malchiodi, E. L., Tormo, J., Schwarz, F. P., and Mariuzza, R. A. (2000) Estimation of the hydrophobic effect in an antigen–antibody protein–protein interface. *Biochemistry* 39, 15375–15387.
78. Manivel, V., Sahoo, N. C., Salunke, D. M., and Rao, K. V. (2000) Maturation of an antibody response is governed by modulations in flexibility of the antigen-combining site. *Immunity* 13, 611–620.